Figure 4.11: The unfiltered ANCORP depth section.

tering in a heterogeneous layer alters the reflected wavefield such that the true shape of a reflector below appears distorted in the seismic image. However, imaging the reflection data in a narrow frequency band, where scattering is less severe than scattering in another frequency band, recovered the true shape of the reflector. This is because the wavefield in heterogeneous media suffers from backscattering and traveltime fluctuations which are frequency dependent.

This section presents the application of the RIS method to the ANCORP data set. The main aim of this study was to extract structural details of the deeper Nazca reflector. The recalculation was performed in three frequency ranges: the low-frequency range between 5 - 10 Hz, the intermediate frequency range between 10 - 15 Hz and the high-frequency range between 15 - 20 Hz. Frequencies lower than 5 Hz were removed during preprocessing of the data. The migration of the filtered data and the stacking of the migrated sections were carried out exactly according to the parameter settings described in section 4.2.2, only the vertical extent of the migration volume was enlarged from 100 km to 130 km.

Results

The unfiltered ANCORP section is shown for comparison in Fig. 4.11. The images obtained by the application of RIS are displayed with the same amplitude scaling. The description of the images focuses on the appearance of the Nazca reflector and the QBBS.

The top section of Fig. 4.12 shows the result for the low-frequency range between 5 - 10 Hz. The dominant wavelength in this case is 500 - 1000 m ($v_p = 5000$ ms^{-1}). The
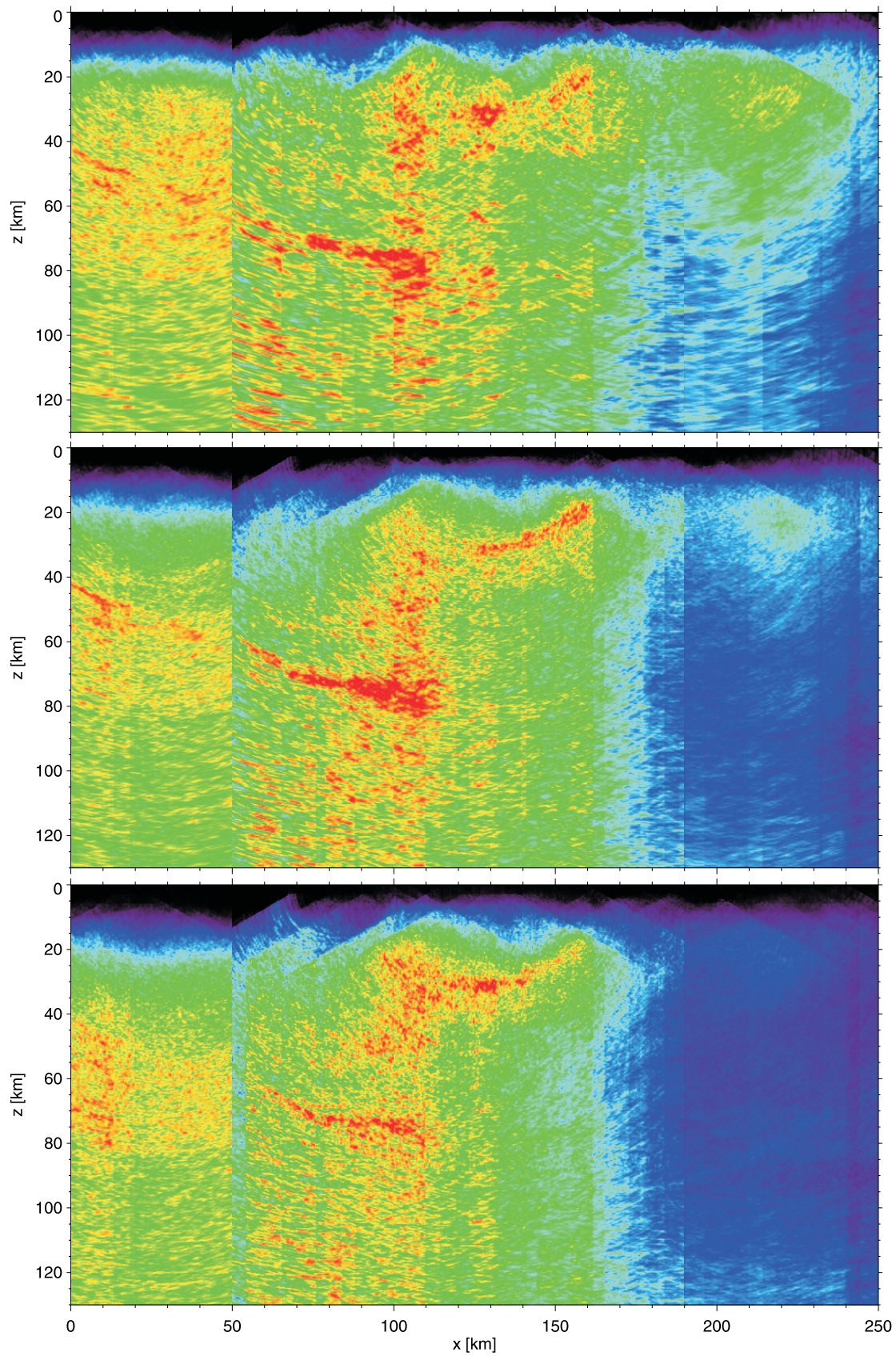
Figure 4.12: The recalculated ANCORP sections in narrow-frequency bands. **Top:** 5 - 10 Hz. **Middle:** 10 - 15 Hz. **Bottom:** 15 - 20 Hz.

width of the normal-incidence Fresnel zone at a depth of 40 km is 6300 - 9000 m, and at a depth of 80 km 9000 - 12600 m, respectively. Between $x = 0$ - 50 km the image is dominated by incoherent reflections at depths between $z = 20$ - 80 km. This region appears heterogeneous and shows a high level of migrated background noise. However, the reflections from the oceanic crust remain relatively sharp and pronounced between $x = 0$ - 20 km. The reflections from the continental Moho are less distinct in comparison to the reflections in the unfiltered section. Between $x = 50$ - 70 km two parallel sharp reflectors are visible at depths between 62 - 75 km. They show the same dip as the reflections at the beginning of the profile. Between $x = 75$ - 82 km the Nazca reflector appears strong with a thickness of about 7 km. The thickness of the Nazca reflector increases from 7 km to ca. 15 km between $x = 72$ - 110 km. The upper boundary of the reflector appears almost horizontal, whereas the lower one dips to the east and becomes blurred at larger depths. At $x = 110$ km the reflectivity suddenly decreases and the shape of the reflector becomes undefined. The reflections between $x = 110$ - 130 km are diffuse and incoherent. The Nazca reflector completely disappears at 130 km. Between $x = 110$ - 160 km the QBBS appears as an incoherent reflection of indistinct shape with varying reflection strength. Between $x = 120$ - 135 km it appears as a 10 - 12 km thick and strong reflector. Between $x = 135$ - 150 km and at depths between 25 - 40 km the QBBS appears distorted and diffuse. Its shape becomes more distinct again between $x = 150$ - 160 km showing a west dipping component. Below the entire QBBS an area of diffuse reflections are visible down to a depth of 40 km. These reflections might indicate that the QBBS only represents the upper boundary of a structure that has a larger vertical extent than previously assumed. West of the QBBS, between $x = 95$ - 120 km a highly reflective region at depths between 20 - 70 km is visible. The reflections in the upper part between depths between 20 - 50 km appear stronger than in the lower part between $x = 50$ - 70 km depth.

The ANCORP image calculated for the frequencies between 10 - 15 Hz is shown in the middle of Fig. 4.12. The dominant wavelengths is 333 - 500 m. Here, the width of the Fresnel zone at depths of 40 km are 5000 - 6300 m, and at a depth of 80 km 7300 - 9000 m, respectively. The reflections from the oceanic crust in the first part of the section ($x = 0$ - 20 km) look similar to the reflections in the low-frequency image. The upper reflections at a depth of 40 km appear pronounced, but the lower reflections are fuzzy and show a less distinct shape. The reflections between $x = 20$ - 50 km become indistinct, only weakly indicating the oceanic crust. The background reflectivity appears decreased in the region below these reflections compared to the low-frequency image. The area above the reflections from the oceanic crust barely shows any reflections. Between $x = 50$ - 65 km the Nazca reflector appears as a ca. 3 km thick reflection band. This reflector merges with

a ca. 5 - 6 km thick reflector at $x = 65$ km. The thickness increases to 15 km between $x = 65$ km and $x = 110$ km. The Nazca reflector appears very strong in this area, but disappears at $x = 115$ km. Between $x = 125$ - 160 km the QBBS is visible as a sharp west dipping reflector. The thickness of the QBBS is about 4 - 6 km along its entire appearance. In a 10 km broad area below the QBBS only weak and incoherent reflections are visible. The heterogeneous region between $x = 90$ - 110 km is dominated by strong, but incoherent reflections. Here, the reflections in the upper part appear weaker than in the lower region. The QBBS appears to be less connected with this region of diffusive reflections compared to the low-frequency image.

The ANCORP data obtained for frequencies between 15 - 20 Hz is shown in the bottom Fig. 4.12. The dominant wavelengths are 250 - 333 m. The widths of the Fresnel zone at a depth of 40 km are 4500 - 5100 m, and at a depth of 80 km 6300 - 7300 m, respectively. The reflections from the oceanic crust appear incoherent and not pronounced ($x = 0$ - 50 km). The background reflectivity appears slightly increased compared to the reflectivity observed in the intermediate-frequency image (Fig. 4.12). At $x = 60$ km thin dipping reflections are visible. They can be tracked down to a depth of 85 km. The upper part of the Nazca reflector shows weak horizontal reflections between $x = 75$ km and $x = 110$ km at depths between 68 - 76 km. Thin dipping reflectors are visible in the lower part of the reflector at depths between 76 - 90 km. The Nazca reflector disappears at $x = 110$ km. In this image the reflectivity of the QBBS changes from east to west. The eastern part of the QBBS ($x = 140$ - 160 km) appears as a weak and diffuse 3 km thick reflection band. Between $x = 110$ - 140 km the reflection strength and the thickness of the reflection band increase. The QBBS appears to be connected with the large vertical scattering region between $x = 90$ - 110 km. Contrary to the intermediate frequency image, this area shows stronger reflectivity in its upper part ($z = 20$ - 50 km) than in the lower part ($z = 50$ - 70 km).

The comparison of all three images shows that the low-frequency image provided the most pronounced and clear reflections from the oceanic crust ($x = 0$ - 50 km). In both other sections these reflections appear less coherent and less pronounced. The distortion of these reflections is strongest in the high frequency image. The low-frequency image reveals sharp reflections from the oceanic crust between $x = 50$ - 70 km of the profile. These reflections are interpreted as the continuation of the oceanic crust visible between $x = 0$ - 20 km. Both other sections only provide pronounced reflections from the top of the oceanic crust, but not from the oceanic Moho. In the low- and in the intermediate frequency image the deep Nazca reflector appear as a large strong reflective area with a maximum height of 15 km between $x = 70$ - 110 km. These images do not reveal structural details within

this region. Contrary to that, the high-frequency image shows thin horizontal as well as parallel dipping reflections in the same area.

The influence of the heterogeneous region above the oceanic crust between $x = 0$ - 20 km on the reflection image appear to be more severe in the high frequency image than in the intermediate- and low-frequency images. Between $x = 70$ - 110 km the situation is vice versa. The high frequencies appear to be less affected by scattering in the overburden, such that the high-frequency image provides a detailed structural image of the deeper parts. These results indicate that scattering is obviously not only dependent on the frequency, but also dependent on the spatial distribution of the heterogeneities within the scattering layer.

The appearance of the QBBS differs in all images. In the intermediate-frequency image the QBBS appears clear and sharp. The low-frequency image of the QBBS is less pronounced, but it indicates that the structure related to the latter is of larger vertical extent than previously assumed. Here, the QBBS appears as an at least 20 km wide and 20 km thick region with a dipping upper boundary. Below the QBBS almost no reflectivity is observed. All images show a 50 km thick highly heterogeneous region between $x = 90$ - 110 km.

In summary, the application of the RIS method on the ANCORP data reveals distinct reflections from the oceanic crust. Parts of these reflections can be traced over a distance of ca. 110 km in all three images. The high-frequency image reveals additional details of the Nazca reflector in the middle of the profile. The low-frequency image indicates that the QBBS is a image of a structure that has a larger vertical extent than previously assumed.

A discussion and interpretation of the results from the recalculation of the ANCORP images using different velocity models (section 4.2.3) and from the application of RIS will be given in the following.

4.2.5 Interpretation and discussion

The results presented in the previous sections provided new insights into the deeper structure of the subduction zone. The ANCORP images using the entire frequency band did not provide explicit reflections from the top or bottom of the oceanic crust below the QBBS in the middle of the profile. From petrophysical and structural considerations the Nazca reflector was interpreted as the image of the hydrated zone in the continental mantle wedge above the oceanic crust (Yuan et al., 2000; ANCORP Working Group, 2003). The

geometry of the oceanic crust itself was derived from the top of the hypocenter locations.

The comparison of the recalculated sections using different velocity models (section 4.2.3) shows that the apparent offset between the Nazca reflector and the hypocenter locations remains independent from the velocity model used for migration of the reflection data. Any of the sections reveals a correlation between the top of the Nazca reflector and the top of the hypocenter locations. From these results it is concluded that the observed offset is real. Interestingly, in the image calculated for the same model used for the localisation of the earthquake hypocenters the Nazca reflector appears more diffuse and disrupted compared to the other images (model 1 and model 3). Also, the image indicates that either the hypocenters are located in the oceanic crust and the continental mantle or that the dip angle of the subducting plate has to decrease at depths larger than 80 km. From both other images indications are given for slightly different, but constant dip angles of the oceanic plate. Thus, these results support the interpretation that the Nazca reflector itself does not image the oceanic crust, but the highly reflective region above it.

Further indications that agree with this interpretation are provided by reflection images calculated using narrow frequency bands of the ANCORP data. The high-frequency image reveals structural details of the Nazca reflector at depths larger than 70 km (Fig. 4.13, top). The image shows thin horizontal as well as east dipping reflections. The horizontal reflections are interpreted as the highly reflective hydrated continental mantle wedge. The dipping reflections shows the same dip as the reflections from the top and bottom of the oceanic crust at the beginning of the profile and between $x = 50 - 70$ km. Also, the depths of these reflections correlate with the prolongated position of the top and bottom reflections from the oceanic crust. Thus, the dipping reflections are interpreted as the oceanic crust. According to this interpretation and considering the uncertainties of the absolute locations of the hypocenters, which are about 3 - 5 km (Rietbrock and Waldhauser, 2004), the hypocenters were located in the oceanic crust and mantle. This result is in agreement with other observations (Bock and Asch, 2000).

In the PRECORP image a similar situation is observed (Fig. 4.13, bottom). Between $x = 45 - 55$ km a short east dipping reflector segment is visible at depths between 60 - 65 km. Also, thin east dipping reflectors at depths larger than 80 km are visible in the middle of the profile ($x = 90 - 120$ km). These reflectors are interpreted as the top and bottom of the oceanic crust. The location of the oceanic crust prolongated in larger depths indicates that the hypocenters are mainly located in the oceanic crust and mantle, except for few outliers. Considering the uncertainty of the absolute vertical position of the hypocenters it can be assumed that the outliers appearing in the continental mantle are
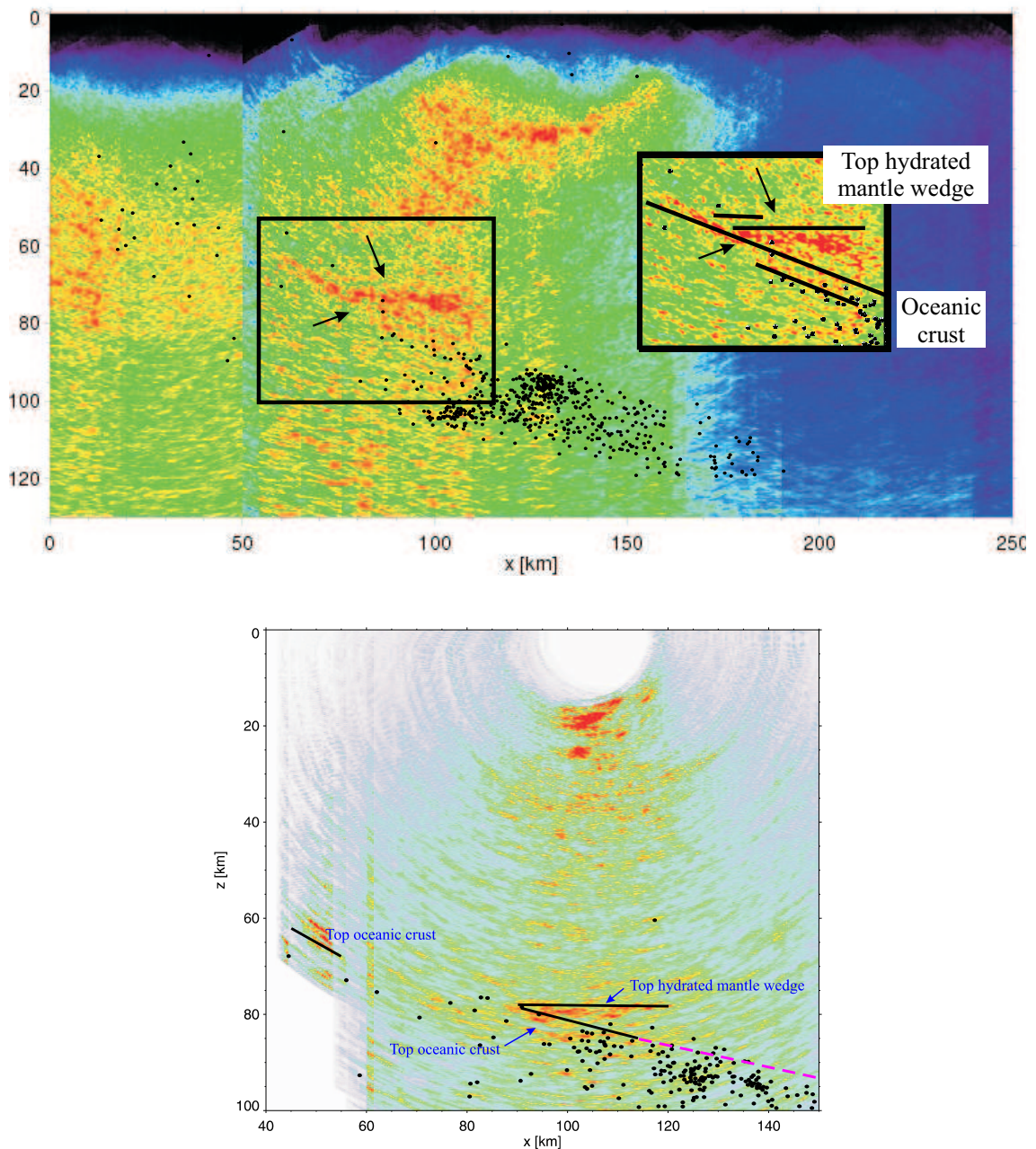
Figure 4.13: **Top:** The high frequency ANCORP image and interpretation (see inset). The horizontal reflections are interpreted as the hydrated continental mantle wedge, the dipping reflections as the oceanic crust. The relocated hypocenter locations are indicated by black dots (Rietbrock and Waldhauser, 2004). **Bottom:** PRECORP depth section and interpretation. The horizontal reflections at depths of 80 km are interpreted as the hydrated mantle wedge, the weaker east dipping reflections at depths larger than 80 km as the oceanic crust (black lines). The black dots represent the hypocenter locations (Gräber and Asch, 1999). The pink dashed line indicates the top of the oceanic crust.

in fact located in the oceanic crust as well. This means that local seismicity is spatially limited to the oceanic crust and the uppermost mantle. In the middle of the PRECORP section at depth of 80 km apparently horizontal reflectors are visible (x =90 - 120 km). These reflectors are interpreted as the highly reflective continental mantle wedge located above the oceanic crust (black line). Compared to the reflectors observed in the ANCORP section these reflectors appear weaker and of less thickness.

Regarding the results from RIS an improved interpretation of the PRECORP section can be presented. The horizontal reflections observed in the middle of the profile at a depth of 80 km are interpreted as the highly reflective continental mantle wedge according the ANCORP image. However, the reflections are thin and weak compared to the strong Nazca reflector in the ANCORP image. Below, thin east dipping reflectors visible at depths larger than 80 km are interpreted as the subducting oceanic crust. The top of the oceanic crust is continued to larger depths with the same dip as observed in the reflection image. This prolongation indicated that the hypocenters are mainly located in the oceanic crust and in the upper mantle. The reported uncertainty of the absolute vertical position of the hypocenters is about 3 - 4 km. Considering this uncertainty it is assumed that the hypocenters in the continental mantle might be located in the oceanic crust as well. Thus, the local seismicity is spatially limited to the oceanic crust and the uppermost mantle.

The unfiltered seismic image reveals the QBBS as a band of distinct west dipping reflections with a thickness of about 10 km. Here, the observed strong reflectivity is interpreted as the presence of partial melts or fluids within the structure. However, results from magnetotelluric data inversion indicate the absence of a good conductor in the corresponding area, thus excluding the existence of a large area of connected fluids and melts. Fig. 4.14 shows two equivalent resistivity models obtained by the inversion of a magnetotelluric data set acquired along the ANCORP profile (pers. comm. Brasse, 2003). In the first model the subducting oceanic crust has not been considered, whereas in the second model the hydrated subducting crust has been implemented as a well conducting body in the inversion process. Independent from the starting model both final sections show a high-resistivity body at almost the same position where the QBBS is located (blue anomaly between x = 130 - 170 km and at depths between 10 - 40 km). However, Schwalenberg et al. (2002) argued that seismic and magnetotelluric observation do not necessarily contradict each other, as the observable high conductivity, other than seismic reflectivity, is dependent on the connectivity of the conducting phase. This might not be existent in this area. The observed strong reflectivity is being related to mafic intrusions into felsic country rocks (ANCORP Working Group, 2003). Furthermore, their modelling studies on the reflection coefficients for an interface between solidified mafic intrusions and felsic
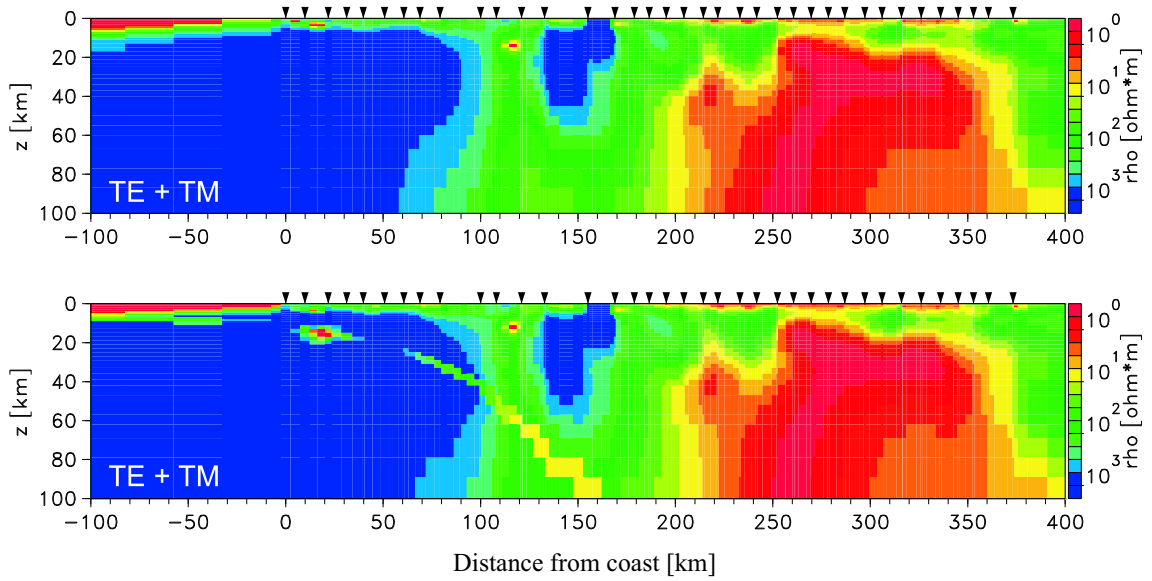
Figure 4.14: Two equivalent resistivity models derived from inversion of magnetotelluric data (pers. comm. Brasse, 2003). The first model did not consider the hydrated oceanic crust, whereas in the second starting model the oceanic crust is considered as a good conductor. Independent from the starting model a body of high resistivity is (blue color observed between $x = 130 - 170$ km at depths between 10 - 40 km.

rocks and the polarity analysis of the seismic records proposed small, regional melt or fluid filled bodies.

The position and the shape of the QBBS visible in the low-frequency image only coincides with the position and the shape of the lower part of the high-resistivity anomaly between $x = 130 - 170$ km and at depths of 10 - 40 km. The QBBS is located between $x = 120 - 160$ km and at depths between 15 - 40 km. Obviously, the structure related to the QBBS cannot simply be correlated to the anomaly visible in the magnetotelluric model.